

The interior structure of rotating black holes 1. Concise derivation

Andrew J S Hamilton^{1,2,*} and Gavin Polhemus^{1,†}

¹*JILA, Box 440, U. Colorado, Boulder, CO 80309, USA*

²*Dept. Astrophysical & Planetary Sciences, U. Colorado, Boulder, CO 80309, USA*

(Dated: November 26, 2024)

This paper presents a concise derivation of a new set of solutions for the interior structure of accreting, rotating black holes. The solutions are conformally stationary, axisymmetric, and conformally separable. Hyper-relativistic counter-streaming between freely-falling collisionless ingoing and outgoing streams leads to mass inflation at the inner horizon, followed by collapse. The solutions fail at an exponentially tiny radius, where the rotational motion of the streams becomes comparable to their radial motion. The papers provide a fully nonlinear, dynamical solution for the interior structure of a rotating black hole from just above the inner horizon inward, down to a tiny scale.

PACS numbers: 04.20.-q

I. INTRODUCTION

Two companion technical papers [1, 2], hereafter Papers 2 and 3, present conformally stationary, axisymmetric, conformally separable solutions for the interior structure of a rotating black hole that accretes a collisionless fluid, undergoes inflation at its inner horizon, and then collapses. Paper 2 deals with uncharged black holes, while Paper 3 generalizes to charged black holes. The purpose of the present paper is to give an abbreviated derivation of the solution for an uncharged black hole, and to summarize the principal features of the solution. A Mathematica notebook containing many details of the calculations is at [3].

The papers consider only classical general relativity, not alternate theories of gravity, nor speculative quantum processes that might occur at the outer horizon.

The Penrose diagram of the analytically extended Kerr [4] geometry, Figure 1, provides a good starting point for understanding where and how the interior Kerr geometry fails. A spherical charged (Reissner-Nordström) black hole has a similar interior structure, with essentially the same Penrose diagram, and much of the literature has focussed on this simpler case. The Kerr geometry, and more generally the Kerr-Newman geometry, has two inner horizons that are gateways to regions of unpredictability, signalled by the presence of timelike singularities. In 1968, Penrose [5] pointed out that an observer passing through the outgoing inner horizon (the Cauchy horizon) of a spherical charged black hole would see the outside Universe infinitely blueshifted, and he suggested that the infinite blueshift would destabilize the inner horizon. The infinite blueshift is plain from the Penrose diagram, Figure 1, which shows that a person passing through the outgoing inner horizon sees the entire future of the outside Universe go by in a finite time. Perturbation theory, much of it expounded in Chandrasekhar’s (1983) monograph [6], confirmed that waves from the outside Universe would amplify to a diverging energy density on the outgoing inner horizon of a spherical charged black hole. The result was widely interpreted as indicating the instability of the inner horizon.

It was not until 1990 that the full nonlinear nature of the instability at the inner horizon was eventually clarified by Poisson & Israel [7]. Poisson & Israel showed that if ingoing and outgoing streams are simultaneously present just above the inner horizon of a spherical charged black hole, then cross-flow between the two streams would lead to an exponential growth of the interior mass. They called the instability “mass inflation.” Shortly thereafter, Barrabès, Israel & Poisson [8] generalized the arguments to the case of rotating black holes, showing that whenever two null sheets cross, an effective mass parameter defined by the product of the expansions of the null bundles inflates. The inflationary instability in spherical charged black holes was confirmed analytically and numerically in several studies, as reviewed by [9].

The physical reason for the inflationary instability can be seen in the Penrose diagram, Figure 1. In the Black Hole region between the outer and inner horizons, the time coordinate (the one that expresses time-translation symmetry) is spacelike, so that it is possible to go either forward or backward in time. Inside the inner horizon, the time coordinate reverts to being timelike. Ingoing particles want to fall into a region where the time coordinate is progressing forwards,

*Electronic address: Andrew.Hamilton@colorado.edu

†Electronic address: Gavin.Polhemus@colorado.edu

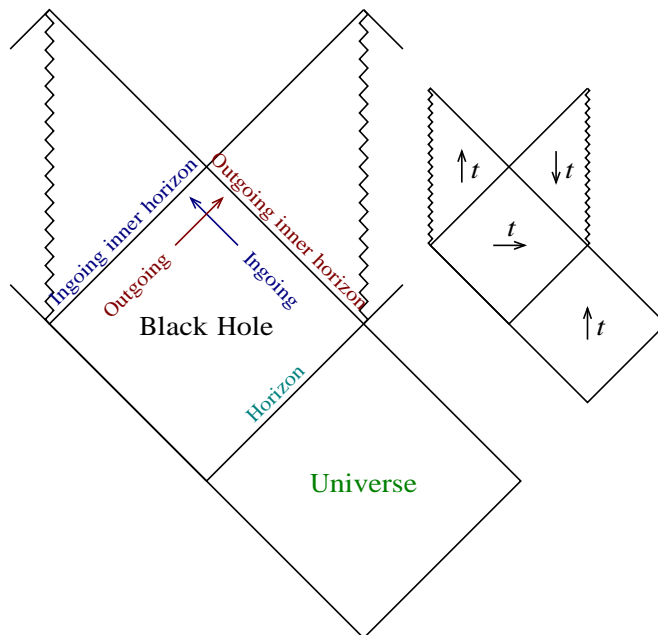


FIG. 1: Partial Penrose diagram illustrating why the Kerr geometry is subject to the inflationary instability. Ingoing and outgoing streams just outside the inner horizon must pass through separate ingoing and outgoing inner horizons into causally separated pieces of spacetime where the timelike Kerr time coordinate t goes in opposite directions. To accomplish this, the ingoing and outgoing streams must exceed the speed of light through each other, which physically they cannot do. In reality, hyper-relativistic counter-streaming between the ingoing and outgoing streams ignites and then drives the exponentially growing inflationary instability. The inset shows the direction of coordinate time t in the various regions. Proper time of course always increases upward in a Penrose diagram.

while outgoing particles want to fall into a region where the time coordinate is progressing backwards. The Penrose diagram, Figure 1, shows that indeed there are two distinct ingoing and outgoing inner horizons which disgorge on to two causally separated pieces of spacetime where the time coordinate is pointed in opposite directions. To achieve this causal separation, the ingoing and outgoing streams must exceed the speed of light relative to each other. This is Penrose's infinite blueshift. In reality, if ingoing and outgoing streams are present, then their attempt to exceed the speed of light relative to each other produces a counter-streaming energy and pressure that, however tiny the initial streams may be, inevitably grows to the point that it becomes a significant source of gravity. As expounded by [9], the counter-streaming pressure produces a gravitational force that is in opposite directions for ingoing and outgoing streams, accelerating the streams ever faster through each other, in turn increasing the counter-streaming pressure. The inflationary instability thus grows exponentially.

II. APPROACH

The strategy adopted in the present papers is motivated by two key physical insights.

The first insight is that, as shown in §V of Paper 2 [1], collisionless ingoing and outgoing streams falling towards the inner horizon of the Kerr-Newman geometry become highly focussed into twin narrow, intense beams pointed along the ingoing and outgoing principal null directions. The focussing is along these two special directions regardless of the initial distributions of orbital parameters of the streams. This implies that the energy-momentum tensor of the ingoing and outgoing streams takes a simple and predictable form near the inner horizon. (We use the term inner horizon to describe the narrow region where inflation takes place, even though the inner horizon is destroyed by inflation, and therefore does not actually exist.)

As first shown by [10], the Kerr-Newman geometry (and some other electrovac geometries) is Hamilton-Jacobi separable in a tetrad aligned with the principal null directions. The fact that collisionless streams focus near the inner horizon along precisely these principal null directions suggests that the spacetime might continue to be separable in the presence of inflation.

The second insight is that the geometry of a spherical charged black hole undergoing inflation at (just above) its inner

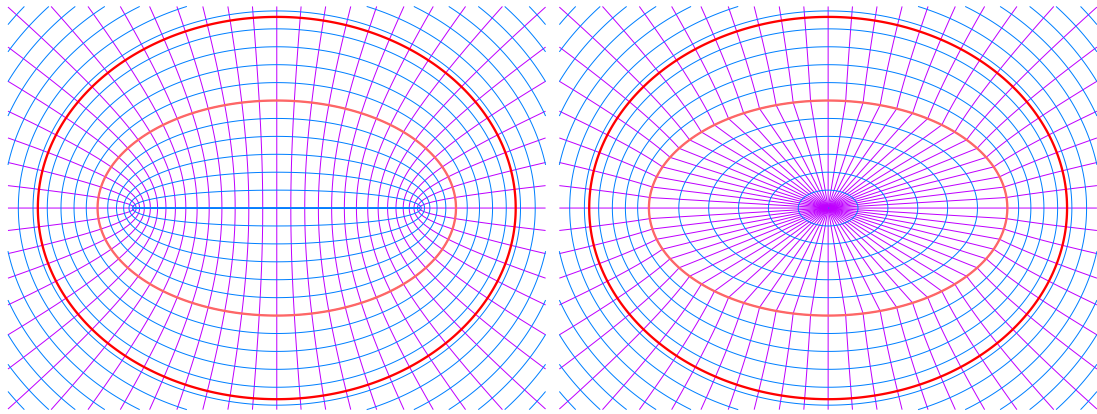


FIG. 2: Contours of constant radius x and latitude y in an uncharged black hole with spin parameter $a = 0.96M_{\bullet}$. The thicker contours mark the outer and inner horizons. The left panel depicts a Kerr black hole. The right panel depicts a black hole of the kind considered in the present series of papers, which undergoes inflation just above the inner horizon, then collapses. In the Kerr geometry, surfaces of constant radius are confocal ellipsoids in Boyer-Lindquist coordinates, while surfaces of constant latitude are confocal hyperboloids, with a ring singularity at their focus. In the inflationary geometry, the streaming energy density and pressure, and Weyl curvature, inflate to exponentially huge values at (just above) the inner horizon, which is destroyed. In the conformally separable solutions presented here, the geometry then collapses radially to exponentially tiny size without changing shape.

horizon has a step-function character. The spacetime is well-approximated by the electrovac (Reissner-Nordström) geometry down to just above the inner horizon. Then, in a tiny interval of radius and proper time near the inner horizon, the centre-of-mass counter-streaming energy and pressure, the Weyl curvature, and the interior mass all inflate to exponentially huge values. Counter-intuitively, the smaller the incident ingoing and outgoing streams, the more rapidly quantities exponentiate [9]. In the limit of tiny accretion rate, the geometry tends to a step-function. This suggests that inflationary spacetimes might be found by looking for solutions with a steplike character. The steplike character of the inflationary solutions can be seen in the sharp turns at the inner horizon in the contours of constant radius and latitude in Figure 2.

As an aside, it is worth commenting on the challenges and pitfalls of computing inflationary spacetimes numerically rather than analytically. One major numerical challenge arises from the fact that during inflation physical quantities inflate to exponentially huge values over tiny intervals of distance and time. One potential pitfall is that inflation requires ingoing and outgoing streams that can stream relativistically through each other. A code, or indeed analytic model, that treats the matter as a single fluid with a sound speed less than the speed of light artificially suppresses inflation by disallowing the relativistic counter-streaming that drives it.

III. SUMMARY DERIVATION

This section summarizes the derivation of the solution for an uncharged rotating black hole. Complete details are given in Paper 2.

The solutions presented in this series of papers are conformally stationary, axisymmetric, and conformally separable. Conformally stationarity combines the assumption of conformal time-translation invariance (self-similarity) with an infinitesimal expansion rate. Let $x^{\mu} \equiv \{x, t, y, \phi\}$ be coordinates in which t is conformal time, ϕ is the azimuthal angle, and x and y are radial and angular coordinates. As shown in Appendix A of Paper 2 [1], the line-element may be taken to be

$$ds^2 = \rho^2 \left[\frac{dx^2}{\Delta_x} - \frac{\Delta_x}{\sigma^4} (dt - \omega_y d\phi)^2 + \frac{dy^2}{\Delta_y} + \frac{\Delta_y}{\sigma^4} (d\phi - \omega_x dt)^2 \right], \quad (1)$$

where

$$\sigma \equiv \sqrt{1 - \omega_x \omega_y}. \quad (2)$$

The determinant of the 2×2 submatrix of t - ϕ metric coefficients defines the radial and angular horizon functions Δ_x

and Δ_y :

$$g_{tt}g_{\phi\phi} - g_{t\phi}^2 = -\frac{\rho^4}{\sigma^4}\Delta_x\Delta_y. \quad (3)$$

Horizons occur when one or other of the horizon functions Δ_x and Δ_y vanish. The focus here is the region near the inner horizon where the radial horizon function Δ_x is negative and tending to zero. The line-element (1) defines a tetrad that is aligned with the principal null directions. Since the radial coordinate x is timelike near the inner horizon, it is convenient to take x as the time coordinate of the tetrad, and to choose the sign of x so that it increases inwards, the direction of advancing time.

The conformal factor ρ is a product of separable (electrovac) ρ_s , time-dependent e^{vt} , and inflationary $e^{-\xi}$ factors,

$$\rho = \rho_s e^{vt-\xi}. \quad (4)$$

Conformal time-translation symmetry is expressed by the fact that the spacetime expands conformally (that is, without changing shape) by factor $\rho \rightarrow e^{v\Delta t}\rho$ when the conformal time increases by $t \rightarrow t + \Delta t$. Conformal stationarity means taking the limit of small expansion rate, or small accretion rate, *after* calculations are complete,

$$v \rightarrow 0. \quad (5)$$

This is not the same as stationarity, which sets v to zero at the outset. A feature of inflation is that the smaller the accretion rate, the faster inflation exponentiates. Even in the limit of infinitesimal accretion rate, inflation drives the centre-of-mass streaming density and pressure, and the Weyl curvature, to exponentially huge values. Mathematically, Einstein's equations contain terms of order $\sim v/\Delta_x$ that grow large at the inner horizon $\Delta_x \rightarrow -0$ however small the accretion rate v may be.

This paper adopts a collisionless fluid as the source of energy-momentum that ignites and then drives inflation. Because collisionless particles stream hyper-relativistically through each other during inflation, the trajectories of massive freely-falling particles are well-approximated by those of massless particles. Conformal separability posits that the equations of motion of freely-falling massless particles are Hamilton-Jacobi separable, which implies that a conformal Killing tensor exists. As shown in Appendix A of Paper 2, conformal separability requires that

$$\begin{aligned} \omega_x, \Delta_x & \text{ are functions of } x \text{ only,} \\ \omega_y, \Delta_y & \text{ are functions of } y \text{ only.} \end{aligned} \quad (6)$$

Unlike strict separability (for massive as well massless particles), conformal separability does not impose conditions on the conformal factor ρ .

Conformally separable inflationary solutions are obtained by separating the Einstein equations systematically. Homogeneous solution of the Einstein components G_{xy} , $G_{t\phi}$, and $G_{xx} + G_{tt}$ and $G_{yy} - G_{\phi\phi}$ leads to the usual electrovac solutions for the electrovac conformal factor ρ_s and the vierbein coefficients ω_x and ω_y :

$$\rho_s = \sqrt{\rho_x^2 + \rho_y^2}, \quad \rho_x = \sqrt{\frac{g_0 - g_1\omega_x}{(f_0g_1 + f_1g_0)(f_0 + f_1\omega_x)}}, \quad \rho_y = \sqrt{\frac{g_1 - g_0\omega_y}{(f_0g_1 + f_1g_0)(f_1 + f_0\omega_y)}}, \quad (7)$$

$$\frac{d\omega_x}{dx} = 2\sqrt{(f_0 + f_1\omega_x)(g_0 - g_1\omega_x)}, \quad \frac{d\omega_y}{dy} = 2\sqrt{(f_1 + f_0\omega_y)(g_1 - g_0\omega_y)}, \quad (8)$$

where f_0 , f_1 , g_0 , and g_1 are constants determined by boundary conditions. Equations (7) and (8) continue to hold throughout inflation and collapse. The inflationary solutions are generic, applying wherever a separable electrovac spacetime has an inner horizon, so the specific choice of constants f_0 , f_1 , g_0 , and g_1 does not affect the argument.

The most important Einstein equations, since they lead to equations governing the evolution of the inflationary exponent ξ and the horizon function Δ_x , are those for the Einstein components $G_{xx} - G_{tt}$ and $G_{yy} + G_{\phi\phi}$. The collisionless source of both these components can be treated as negligible, in the conformally stationary limit of small accretion rate. The angular components are negligible because inflation amplifies the radial, not angular components; and the trace of the collisionless energy-momentum remains small because it depends on the rest mass of the particles, which is unchanged by inflation. Define U_x , U_y , X_x , X_y , Y_x , and Y_y by

$$U_x \equiv -\frac{\partial\xi}{\partial x}\Delta_x, \quad U_y \equiv \frac{\partial\xi}{\partial y}\Delta_y, \quad (9a)$$

$$X_x \equiv \frac{\partial U_x}{\partial x} + 2\frac{U_x^2 - v^2}{\Delta_x}, \quad X_y \equiv \frac{\partial U_y}{\partial y} - 2\frac{U_y^2 + v^2\omega_y^2}{\Delta_y}, \quad (9b)$$

$$Y_x \equiv \frac{d\Delta_x}{dx} + 3U_x - \Delta_x \frac{d}{dx} \ln \left[(f_0 + f_1\omega_x) \frac{d\omega_x}{dx} \right], \quad Y_y \equiv \frac{d\Delta_y}{dy} - 3U_y - \Delta_y \frac{d}{dy} \ln \left[(f_1 + f_0\omega_y) \frac{d\omega_y}{dy} \right]. \quad (9c)$$

In terms of these quantities, the Einstein components $G_{xx} - G_{tt}$ and $G_{yy} + G_{\phi\phi}$ are

$$\begin{aligned} \rho^2 (G_{xx} - G_{tt}) &= \frac{1}{\sigma^2} \left(Y_x \frac{d \ln \omega_x}{dx} - Y_y \frac{d \ln \omega_y}{dy} \right) - 2X_x + Y_x \frac{d}{dx} \ln \left(\frac{f_0 + f_1 \omega_x}{\omega_x} \right) + X_y - \frac{\partial Y_y}{\partial y} + Y_y \frac{d}{dy} \ln \left[\frac{\omega_y (f_1 + f_0 \omega_y)}{d\omega_y/dy} \right] \\ &\quad + U_x \frac{\partial}{\partial x} \ln [\sigma^2 (f_0 + f_1 \omega_x)] - U_y \frac{\partial}{\partial y} \ln \left[\frac{(g_1 - g_0 \omega_y) d\omega_y}{\sigma^2 dy} \right], \end{aligned} \quad (10a)$$

$$\begin{aligned} \rho^2 (G_{yy} + G_{\phi\phi}) &= \frac{1}{\sigma^2} \left(Y_x \frac{d \ln \omega_x}{dx} - Y_y \frac{d \ln \omega_y}{dy} \right) - 2X_y - Y_y \frac{d}{dy} \ln \left(\frac{f_1 + f_0 \omega_y}{\omega_y} \right) + X_x + \frac{\partial Y_x}{\partial x} - Y_x \frac{d}{dx} \ln \left[\frac{\omega_x (f_0 + f_1 \omega_x)}{d\omega_x/dx} \right] \\ &\quad + U_y \frac{\partial}{\partial y} \ln [\sigma^2 (f_1 + f_0 \omega_y)] - U_x \frac{\partial}{\partial x} \ln \left[\frac{(g_0 - g_1 \omega_x) d\omega_x}{\sigma^2 dx} \right]. \end{aligned} \quad (10b)$$

Homogeneous solutions of these equations can be found by supposing that U_x , X_x , and Y_x are all functions of radius x , while U_y , X_y , and Y_y are all functions of radius y , and by separating each of the equations as

$$\frac{1}{\sigma^2} \left(\frac{f_0 h_0 + h_2 \omega_x + f_1 h_1 \omega_x^2}{\omega_x} - \frac{f_1 h_1 + h_2 \omega_y + f_0 h_0 \omega_y^2}{\omega_y} \right) - \frac{f_0 h_0 + h_3 \omega_x}{\omega_x} + \frac{f_1 h_1 + h_3 \omega_y}{\omega_y} = 0, \quad (11)$$

for some constants h_0 , h_1 , h_2 , and h_3 . If one attempts to separate equations (10) exactly, then the attempt fails unless U_x and U_y are identically zero, which is the usual electrovac case. But if U_x is taken to be small but finite, then separation succeeds, and inflation emerges. If U_x and U_y on the second lines of equations (10) are treated as negligibly small, then separating the first lines of each of equations (10) according to the pattern of equation (11) leads to the homogeneous solutions

$$X_x = 0, \quad X_y = 0, \quad (12a)$$

$$Y_x = \frac{(f_0 + f_1 \omega_x)(h_0 + h_1 \omega_x)}{d\omega_x/dx}, \quad Y_y = \frac{(f_1 + f_0 \omega_y)(h_1 + h_0 \omega_y)}{d\omega_y/dy}. \quad (12b)$$

If $U_x = U_y = 0$, then solution of equations (9c) and (12b) for Y_x and Y_y , subject to appropriate boundary conditions, yields the radial and angular horizon functions Δ_x and Δ_y of the Kerr line-element. The result is easily generalized to other electrovac spacetimes by admitting appropriate sources for Y_x and Y_y .

The quantity X_y defined by equation (9b) determines the evolution of U_y , and the solution $X_y = 0$, equation (12a), then implies that inflation leaves U_y unchanged, and sensibly equal to its electrovac value of zero, in the conformally stationary limit. Thus inflation leaves the angular horizon function Δ_y unchanged from its electrovac value.

On the other hand, inflation drives U_x away from zero however small it might initially be. In the vicinity of the inner horizon, where $\Delta_x \rightarrow -0$, the solutions (12) for X_x and Y_x defined by equations (9b) and (9c) imply the evolution equations

$$\frac{\partial U_x}{\partial x} + 2 \frac{U_x^2 - v^2}{\Delta_x} = 0, \quad (13a)$$

$$\frac{d\Delta_x}{dx} + 3U_x = \Delta'_x, \quad (13b)$$

where $\Delta'_x \equiv d\Delta_x/dx|_{x_{\text{in}}}$ is the (positive) derivative of the electrovac horizon function at the inner horizon $x = x_{\text{in}}$. Below, equation (28c), it will be found that the radius x remains frozen at its inner horizon value x_{in} throughout inflation and collapse, so the right hand side of equation (13b), which is the electrovac solution for Y_x evaluated at the inner horizon, is constant during inflation and collapse. The evolution equation (13a) for U_x involves a term inversely proportional to the horizon function Δ_x , which diverges at the inner horizon $\Delta_x \rightarrow -0$, driving U_x away from zero however small U_x might initially be.

Equation (13a) leads to instability only at the inner horizon, where $\Delta_x \rightarrow -0$. At the outer horizon, where $\Delta_x \rightarrow 0$, solutions of equation (13a) decay rather than grow.

The separation of the Einstein components (10) that leads to the evolution equations (13) was premised on the assumption that the terms proportional to U_x and U_y on the second lines of equations (10) could be neglected. However, the separation continues to remain valid during inflation and collapse when U_x grows huge. The reason for this is that the dominant terms in the Einstein components (10) during inflation and collapse are of order U_x^2/Δ_x , coming from the expression (9b) for X_x . Thus, once U_x ceases to be negligible, the condition for the validity of the separation becomes $U_x \ll U_x^2/|\Delta_x|$, or equivalently $|\Delta_x| \ll U_x$. Consequently the condition for the validity of the separation of the Einstein components (10) is

$$\text{either } U_x \ll 1 \quad \text{or} \quad |\Delta_x| \ll U_x. \quad (14)$$

Condition (14) holds from electrovac through inflation and collapse, provided that the accretion rate is small, as conformal stationarity prescribes. The fact that condition (14) suffices is verified in §VIII J of Paper 2, where the Einstein equations are solved to next order in Δ_x/U_x , and it is shown that the effect on the evolution of the inflationary exponent ξ and horizon function Δ_x is negligible.

The evolution equations (13) are solved in the next section, §IV, but first it is necessary to attend to the other Einstein equations.

In the conformally separable geometry, freely-falling collisionless ingoing and outgoing streams become highly focussed along the principal ingoing and outgoing null directions as they approach the inner horizon. Inflation accelerates the streams even faster along the same null directions, causing the x and t components of the tetrad-frame momenta of freely-falling collisionless streams to grow exponentially. Consequently the collisionless energy-momentum is dominated by its x - t components. The associated components of the Einstein tensor are

$$\rho^2 \left(\frac{G_{xx} + G_{tt}}{2} \pm G_{xt} \right) = (U_x \mp v) \left[\frac{Y_x \pm v}{-\Delta_x} - \frac{d}{dx} \ln \left(\frac{d\omega_x}{dx} \right) \right] + X_x . \quad (15)$$

Since $X_x = 0$, and $Y_x = \Delta'_x$, and the term proportional to $d \ln(d\omega_x/dx)/dx$ is sub-dominant (in fact the term disappears when the Einstein components (10) and corresponding evolution equations (13) are solved to next order in Δ_x/U_x ; see Paper 2), equation (15) simplifies to

$$\rho^2 \left(\frac{G_{xx} + G_{tt}}{2} \pm G_{xt} \right) = \frac{1}{-\Delta_x} (U_x \mp v) (\Delta'_x \pm v) . \quad (16)$$

The right hand side of equation (15) agrees with 8π times the energy-momentum tensor of two collisionless streams, one ingoing (+) and one outgoing (-),

$$T_{kl} = N^+ p_k^+ p_l^+ + N^- p_k^- p_l^- , \quad (17)$$

with densities

$$N^\pm = \frac{1}{16\pi} (U_x \mp v) (\Delta'_x \pm v) , \quad (18)$$

and tetrad-frame momenta

$$p_k^\pm = \frac{1}{\rho} \left\{ -\frac{1}{\sqrt{-\Delta_x}}, \mp \frac{1}{\sqrt{-\Delta_x}}, 0, 0 \right\} . \quad (19)$$

The tetrad-frame momenta (19) are null vectors pointed along the principal ingoing and outgoing null directions. That equations (18) and (19) describe correctly the behaviour of freely-falling streams can be shown by solving the Hamilton-Jacobi and collisionless Boltzmann equations (see Paper 2), and can be confirmed by checking that the densities and momenta satisfy, to requisite accuracy, covariant number conservation, $D^k N^\pm p_k^\pm = 0$, and the geodesic equation $dp_k^\pm/d\lambda = 0$, where λ is an affine parameter. It might seem somewhat miraculous that the x - t components of the Einstein equations are satisfied with a collisionless source, but it is no coincidence. Einstein's equations enforce covariant energy-momentum conservation, $D^k T_{kl} = 0$. Since the angular components are sub-dominant, only the 3 distinct x - t components of the energy-momentum tensor are important. The 3 components are subject to 2 energy-momentum conservation equations, but in the present instance the 2 conservation equations are redundant, so there is effectively 1 conservation equation. However, the energy-momentum conservation equations for freely-falling ingoing and outgoing streams are symmetrically related to each other by $v \rightarrow -v$, so conservation of the sum of their energies, as enforced by Einstein, implies conservation of both. The two conservation equations, coupled with solution of the Einstein equation for $G_{xx} - G_{tt}$, equation (10a), leads to a complete, self-consistent set of equations.

The angular motions of the freely-falling streams are small compared to their radial motions, but not necessarily zero. Next in order of magnitude, after the 3 radial (x - t) components of the energy-momentum tensor, are its 4 off-diagonal radial-angular components. The corresponding components of the Einstein tensor are

$$\rho^2 (G_{xy} \pm G_{ty}) = -\frac{1}{\sqrt{-\Delta_x \Delta_y}} (U_x \mp v) \left(\Delta_y \frac{\partial \ln \rho_s^2}{\partial y} - 2U_y \right) - \sqrt{\frac{-\Delta_x}{\Delta_y}} \left(U_y \frac{\partial \ln \rho_s^2}{\partial x} \pm \frac{v\omega_y}{\sigma^2} \frac{d\omega_y}{dy} \right) , \quad (20a)$$

$$\rho^2 (G_{x\phi} \pm G_{t\phi}) = \pm \frac{1}{\sqrt{-\Delta_x \Delta_y}} (U_x \mp v) \left(\frac{\Delta_y}{\sigma^2} \frac{d\omega_x}{dx} \mp 2v\omega_y \right) \mp \sqrt{\frac{-\Delta_x}{\Delta_y}} \left(\frac{U_y}{\sigma^2} \frac{d\omega_y}{dy} \mp v\omega_y \frac{\partial \ln \rho_s^2}{\partial x} \right) . \quad (20b)$$

Since U_y and the terms proportional to $v\sqrt{-\Delta_x}$ are negligible, equations (20) simplify to

$$\rho^2 (G_{xy} \pm G_{ty}) = -\frac{1}{\sqrt{-\Delta_x \Delta_y}} (U_x \mp v) \Delta_y \frac{\partial \ln \rho_s^2}{\partial y}, \quad (21a)$$

$$\rho^2 (G_{x\phi} \pm G_{t\phi}) = \pm \frac{1}{\sqrt{-\Delta_x \Delta_y}} (U_x \mp v) \left(\frac{\Delta_y \omega'_x}{\sigma^2} \mp 2v\omega_y \right), \quad (21b)$$

where $\omega'_x \equiv d\omega_x/dx|_{x_{\text{in}}}$, which is effectively constant throughout inflation and collapse, is the derivative of ω_x at the inner horizon $x = x_{\text{in}}$, equation (8). The right hand sides of equations (21) agree with 8π times the energy-momentum tensor of ingoing and outgoing streams with the same densities N^\pm as before, equation (18), but with tetrad-frame momenta p_k^\pm having finite rather than zero angular components:

$$p_k^\pm = \frac{1}{\rho} \left\{ -\frac{1}{\sqrt{-\Delta_x}}, \mp \frac{1}{\sqrt{-\Delta_x}}, \frac{1}{\sqrt{\Delta_y}} \left(\frac{\Delta_y \partial \ln \rho_s^2 / \partial y}{\Delta'_x \pm v} \right), \mp \frac{1}{\sqrt{\Delta_y}} \left(\frac{\Delta_y \omega'_x / \sigma^2 \mp 2v\omega_y}{\Delta'_x \pm v} \right) \right\}. \quad (22)$$

The tetrad-frame momenta (22) satisfy the Hamilton-Jacobi equations with constant Hamilton-Jacobi parameters along the path of the streams. The angular components of the momenta are small compared to the radial components as long as

$$|\Delta_x| \ll 1. \quad (23)$$

The momentum (22) is hyper-relativistic, and $p_t^\pm = \pm p_x^\pm$ to an excellent approximation so long as condition (23) is true. If the condition (23) is violated, then it signifies that angular motions are becoming important, and the solution is breaking down.

It should be emphasized that, as long as condition (23) holds, the purely radial (x - t) Einstein equations hold regardless of angular motions, and thus the radial solution is unaffected by angular motions. However, if one requires that the sub-dominant radial-angular Einstein equations are also satisfied, then the angular motion of the collisionless streams must be as given by equation (22). One might perhaps have expected that conformally separable solutions would require that the collisionless streams would move exactly along the principal null directions, but equation (22) shows that this is not true.

Again, it might seem remarkable that the radial-angular Einstein equations are satisfied by collisionless ingoing and outgoing streams. And again, this coincidence results from energy-momentum conservation. There are 4 radial-angular Einstein components, subject to 2 energy-momentum conservation equations. The energy-momentum conservation equations for the freely-falling ingoing and outgoing streams are symmetrically related by $v \rightarrow -v$, so conservation of their sum implies conservation of both.

The final, sub-sub-dominant, components of the energy-momentum tensor are the 3 purely angular (y - ϕ) components. The component $G_{yy} + G_{\phi\phi}$ component has already been addressed, equation (10b). The remaining 2 components are

$$\rho^2 \left(\frac{G_{yy} - G_{\phi\phi}}{2} \pm iG_{y\phi} \right) = (U_y \mp iv\omega_y) \left[\frac{-Y_y \pm iv\omega_y}{\Delta_y} - \frac{d}{dy} \ln \left(\frac{d\omega_y}{dy} \right) \right] + X_y \mp iv \frac{d\omega_y}{dy}. \quad (24)$$

Since $X_y = 0$, and U_y and v are negligibly small, and there are no denominators of the radial horizon function Δ_x , equation (24) simplifies to

$$\rho^2 \left(\frac{G_{yy} - G_{\phi\phi}}{2} \pm iG_{y\phi} \right) = 0. \quad (25)$$

During inflation, the collisionless streams have negligible angular components of energy-momentum because the densities of the accreting streams are negligible, in the conformally stationary limit, and inflation does not amplify angular motions. During collapse, the conformal factor ρ shrinks, and angular motions grow. However, as long as the angular motions are sub-dominant, which is true as long as condition (23) is satisfied, the angular components of the energy-momentum can be neglected consistently: the Einstein equations for the purely radial components, and for the radial-angular components, are unaffected by the angular components (25) (the angular component $G_{yy} + G_{\phi\phi}$, along with $G_{xx} - G_{tt}$, equations (10), determined the angular horizon function Δ_y , which inflation leaves unaltered from its electrovac form). Equation (25) requires that the 2×2 angular submatrix of the energy-momentum tensor be isotropic, proportional to the 2×2 unit matrix. As discussed in Paper 2, it is possible to arrange the angular energy-momentum to be isotropic by admitting multiple ingoing and outgoing streams, with mean momenta set by equation (22) and isotropic mean squared momenta. Treating the diagonal components of the angular energy-momentum requires taking equations (10) to next order in Δ_x/U_x , but this can be done.

Eventually however, the angular components do become important, when $|\Delta_x| \sim 1$, and the solution fails.

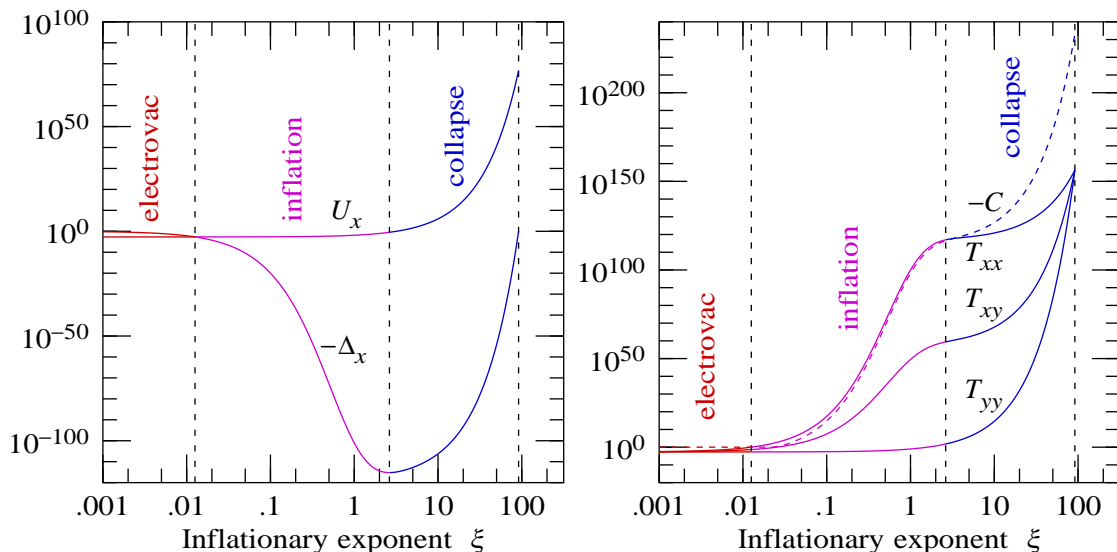


FIG. 3: Evolution of the geometry and energy-momenta from electrovac through inflation and collapse. (Left) The parameter $U_x \equiv -\Delta_x d\xi/dx$ and the horizon function Δ_x , equations (28), as a function of the inflationary exponent ξ , for parameters $v = 0.001$, $u = 0.002$, and $\Delta'_x = 1$ (the solutions in this paper apply in the limit of tiny v and u ; small finite values are adopted in this plot to avoid numerical overflow). Inflation ignites as the horizon function $|\Delta_x|$ decreases below U_x . Inflation ends as the absolute value of the horizon function goes through a minimum, and the geometry proceeds to collapse. Once $|\Delta_x| \gtrsim 1$, the angular components of the collisionless streams exceed their radial components, and the solution breaks down, but this happens only after the geometry has collapsed to exponentially tiny scale. (Right) The tetrad-frame radial, radial-angular, and angular collisionless energy-momenta $T_{xx} \propto \rho^{-2} U_x / |\Delta_x|$, $T_{xy} \propto \rho^{-2} U_x / \sqrt{|\Delta_x|}$, and $T_{yy} \propto \rho^{-2} U_x$. The energy-momenta grow exponentially huge despite their small initial values. Indeed, the smaller the initial energy-momenta, the faster and larger they grow. The dashed line is minus the polar (real) spin-0 component of the Weyl curvature, $-C \propto \rho^{-2} U_x^2 / |\Delta_x|$. The axial (imaginary) spin-0 Weyl component is comparable to T_{yy} .

IV. INFLATION AND COLLAPSE

Denote the initial value of U_x , equation (9a), incident on the inner horizon by u , a small parameter of order v ,

$$U_x = u \quad \text{initially} . \quad (26)$$

The densities N^\pm of ingoing and outgoing streams incident on the inner horizon are proportional to $u \mp v$, equation (18). Inflation is driven by counter-streaming between ingoing and outgoing streams, so both streams must be present for inflation to occur, but even the tiniest amount suffices to trigger inflation. Positivity of both ingoing and outgoing densities requires that

$$u > v > 0 , \quad (27)$$

the condition $v > 0$ coming from the fact that the black hole must expand as it accretes. The case $v = 0$ is the stationary (or homogeneous) approximation of [11]. The densities N^\pm , equation (18), are also proportional to $\Delta'_x \mp v$, where Δ'_x is the positive derivative of the electrovac horizon function at the inner horizon. Positivity of both ingoing and outgoing densities requires Δ'_x to be strictly positive, which excludes extremal black holes, whose inner and outer horizons coincide, and which have $\Delta'_x = 0$ at the horizon.

Solution of the evolution equations (13) for U_x and Δ_x yields

$$U_x = \sqrt{v^2 + (u^2 - v^2)e^{4\xi}} , \quad (28a)$$

$$\Delta_x = - \left(\frac{U_x^2 - v^2}{u^2 - v^2} \right)^{3/4} \left[\frac{(U_x + v)(u - v)}{(U_x - v)(u + v)} \right]^{\Delta'_x/(4v)} , \quad (28b)$$

$$x - x_{\text{in}} = - \int \frac{\Delta_x dU_x}{2(U_x^2 - v^2)} . \quad (28c)$$

The integral on the right hand side of equation (28c) can be expressed analytically as an incomplete beta function, but the expression is not useful. Physically, equation (28c) says that the radius x is frozen at its inner horizon value x_{in} during inflation and collapse, where U_x is growing, while Δ_x remains small.

Figure 3 illustrates the evolution of U_x and the horizon function Δ_x as a function of the inflationary exponent ξ , for parameters $v = 0.001$ and $u = 0.002$. The value $v = 0.001$, which physically represents the velocity with which a distant observer sees the characteristic radius of the black hole expand, is large compared to a typical astronomical accretion rate, but a large value is needed to avoid numerical overflow. Inflation ignites near the inner horizon as the horizon function $|\Delta_x|$ drops below u . During inflation, the horizon function $|\Delta_x|$ decreases exponentially, while U_x increases slowly. During inflation, the inflationary exponent ξ in the conformal factor ρ , equation (4), satisfies

$$\xi \ll \frac{d\xi}{dx} \ll \frac{d^2\xi}{dx^2}, \quad (29)$$

which is the behaviour characteristic of a step-function. The inequalities (29) essentially say that the acceleration $d^2\xi/dx^2$ of the inflationary exponent, which is driven by the radial energy-momentum of the collisionless streams, is much larger than the velocity $d\xi/dx$, which in turn is much larger than the distance moved ξ .

Inflation ends when the absolute value of the horizon function reaches a minimum, at an exponentially tiny value,

$$|\Delta_x| \sim e^{-1/v}, \quad (30)$$

at which point the spacetime collapses. During collapse, the horizon function $|\Delta_x|$ increases, while the conformal factor $\rho \propto e^{-\xi}$ shrinks exponentially, no longer satisfying the inequalities (29). The radial coordinate x remains frozen even while the conformal factor ρ is shrinking. That the spacetime collapses rather than leads to a null singularity accords with the conclusion of [9] that the outcome of inflation is collapse when a black hole continues to accrete, as is ensured in the present case by the assumption of conformal time translation invariance (self-similarity).

During collapse the horizon function increases back to of order unity, $|\Delta_x| \sim 1$. At this point the angular motion of the freely-falling ingoing and outgoing streams becomes comparable to their radial motion, and the solution breaks down. This happens when the conformal factor has collapsed to an exponentially tiny value,

$$\rho \sim e^{-1/v}. \quad (31)$$

The right panel of Figure 3 shows the magnitudes of the radial, radial-angular, and angular components T_{xx} , T_{xy} , and T_{yy} of the tetrad-frame energy-momenta of the collisionless streams. During inflation, the radial energy-momentum grows fastest, reaching an exponentially huge value

$$T_{xx} \sim e^{1/v}. \quad (32)$$

During collapse, the angular energy-momentum grows fastest.

The Weyl curvature tensor has only a spin-0 component, which classifies the spacetime as Petrov Type D. The right panel of Figure 3 shows minus the polar (real) part of the spin-0 component of the Weyl curvature.

It is notable that the smaller the accretion rate v , the more rapidly inflation exponentiates, and the larger the energy-momentum and curvature grow, in agreement with the conclusions of [9, 12].

V. BOUNDARY CONDITIONS

The solutions are determined by boundary conditions of the collisionless streams incident on the inner horizon. Since the solution above the inner horizon is well-approximated by the Kerr (or other electrovac) solution, the behaviour of gas above the inner horizon does not affect the solution.

The requirement of conformal separability imposes special boundary conditions. The densities N^\pm of ingoing (+) and outgoing (−) streams incident on the inner horizon are, equation (18), since $U_x = u$ initially,

$$N^\pm = \frac{1}{16\pi}(u \mp v)(\Delta'_x \pm v). \quad (33)$$

This is just a constant, independent of angular position on the inner horizon. Thus conformal separability requires that the incident flow of ingoing and outgoing streams be “monopole,” independent of latitude. It makes physical sense that conformal separability would require this high degree of symmetry of the accretion flow.

As emphasized in §III, because the radial motions of collisionless streams dominate their angular motions during inflation and collapse (up until the angular motions become important, at $|\Delta_x| \sim 1$), the radial Einstein equations

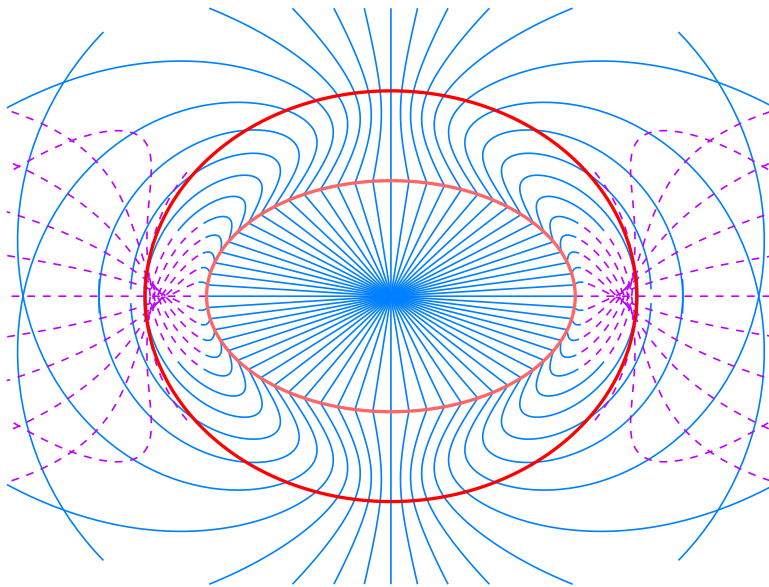


FIG. 4: Angular flow pattern of freely-falling particles that produces the conditions (22) at the inner horizon required if conformal separability is imposed to sub-dominant radial-angular order, for an uncharged black hole with spin parameter $a = 0.96M_{\bullet}$. The thicker contours mark the outer and inner horizons, the latter being destroyed by inflation. Ingoing and outgoing particles fall along the same trajectories in the x - y plane, but have opposite motions in the azimuthal ϕ coordinate. Trajectories near the equatorial plane change from ingoing to outgoing, or vice versa, inside the outer horizon; the transition is marked by the lines changing from dashed to solid. The angular flow pattern cannot be achieved with collisionless streams that fall from outside the outer horizon. In the equatorial region, outgoing but not ingoing particles can fall from outside the outer horizon, while in the polar region, ingoing but not outgoing particles can fall from outside the outer horizon.

are unaffected by the angular motion, and the boundary condition (33) is all that is needed to ensure conformal separability with sufficient accuracy. However, if it is required that the sub-dominant radial-angular components of the Einstein equations are also satisfied, which is a more stringent constraint on conformal separability, then the tetrad-frame momenta p_k^{\pm} of the streams must have finite angular components, satisfying equation (22). Figure 4 illustrates the required flow pattern for a black hole of spin parameter $a = 0.96M_{\bullet}$. The energy per unit mass of infalling particles, which is unspecified by boundary conditions, is chosen here to be $E/m = \pm 1$.

As described in Paper 2, the required angular flow pattern cannot be achieved with collisionless streams falling from outside the outer horizon. Streams that fall from outside the outer horizon must necessarily be ingoing at the outer horizon, which eliminates half the phase space available to collisionless streams, making it impossible to satisfy the required conditions on the angular motion of the streams. Thus, if the angular conditions are imposed, then the collisionless ingoing and outgoing streams must be considered as being delivered ad hoc to just above the inner horizon.

VI. CONCLUSION

This paper has presented conformally stationary, axisymmetric, conformally separable solutions for the interior structure of an uncharged rotating black hole that undergoes inflation just above its inner horizon, then collapses. It has long been known that linear perturbations diverge at the inner horizon of the Kerr geometry, and it has been suspected that perturbations would develop nonlinearly similarly to the inflationary instability [7] known to operate in spherical charged black holes [9], and expected to occur also in rotating black holes [8]. The self-consistent nonlinear solutions found here confirm that, at least in the conformally separable special case considered here, the inflationary instability develops in rotating black holes as anticipated.

A feature of the Kerr geometry (and other separable electrovac geometries) is that, as freely-falling ingoing and outgoing particles approach the inner horizon, they become highly focussed along the ingoing and outgoing null directions, regardless of their initial angular motion. However small the accretion rate may be, eventually the energy and pressure of the twin beams of particles counter-streaming hyper-relativistically along the ingoing and outgoing null directions grows large enough to be a source of gravity. The gravity produced by the counter-streaming acts

to accelerate ingoing and outgoing stream even faster through each other, leading to an exponential growth in the streaming density and pressure, and in the curvature. This is inflation. The huge gravitational acceleration produced by the counter-streaming is in the inward direction, to smaller radius, but each stream thinks that they are moving in the inward direction, so the streams are accelerated in opposite directions.

Inflation takes place over an extremely short interval of proper time. Inflation is like a bullet fired in the chamber of a gun: an explosion accelerates the bullet, and shortly after the bullet achieves high velocity, but still the bullet has hardly moved (see the inequalities (29)). Inflation does in due course alter the geometry, but in a predictable way: the conformal factor, having been accelerated to huge velocity inward, proceeds to shrink rapidly. The geometry collapses.

During inflation, the ingoing and outgoing streams were accelerated along the principal null directions, without amplifying the angular motion. During collapse, the angular motions grow. At an exponentially tiny scale, the angular motions become comparable to the radial motion, and the solutions considered in this paper break down. What happens then is undetermined.

The existence of conformally separable solutions for the inflationary zones of rotating black holes is not surprising. Ingoing and outgoing streams focus along the principal null directions as they approach the inner horizon, and the streaming energy and pressure generated by the radial beams accelerates the streams along the same null directions. The acceleration depends on the accretion rate. If the densities of ingoing and outgoing streams incident on the inner horizon are uniform, independent of latitude, then inflation accelerates the beams at the same rate at all latitudes. When the geometry begins to collapse, it does so uniformly, preserving conformal separability. What happens in the more general case when the accretion flow on to the inner horizon varies with angular position remains to be seen. But that inflation will occur is physically inevitable.

Acknowledgments

This work was supported by NSF award AST-0708607.

References

-
- [1] Andrew J. S. Hamilton. The interior structure of rotating black holes II. Uncharged black holes. *Phys. Rev.*, D84:124056, 2011.
 - [2] Andrew J. S. Hamilton. The interior structure of rotating black holes III. Charged black holes. *Phys. Rev.*, D84:124057, 2011.
 - [3] Andrew J. S. Hamilton. Mathematica notebook on rotation inflationary spacetimes. <http://jila.colorado.edu/~ajsh/rotatinginflationary/rotatinginflationary.nb>, 2011.
 - [4] Roy P. Kerr. Gravitational field of a spinning mass as an example of algebraically special metrics. *Phys. Rev. Lett.*, 11:237–238, 1963.
 - [5] Roger Penrose. Structure of space-time. In Cécile de Witt-Morette and John A. Wheeler, editors, *Battelle Rencontres: 1967 lectures in mathematics and physics*, pages 121–235. W. A. Benjamin, New York, 1968.
 - [6] Subrahmanyan Chandrasekhar. *The mathematical theory of black holes*. Clarendon Press, Oxford, England, 1983.
 - [7] E. Poisson and W. Israel. Internal structure of black holes. *Phys. Rev.*, D41:1796–1809, 1990.
 - [8] C. Barrabès, W. Israel, and E. Poisson. Collision of light-like shells and mass inflation in rotating black holes. *Class. Quant. Grav.*, 7(12):L273–L278, 1990.
 - [9] Andrew J. S. Hamilton and Pedro P. Avelino. The physics of the relativistic counter-streaming instability that drives mass inflation inside black holes. *Phys. Rept.*, 495:1–32, 2010.
 - [10] Brandon Carter. Hamilton-Jacobi and Schrödinger separable solutions of Einstein's equations. *Commun. Math. Phys.*, 10:280–310, 1968.
 - [11] Lior M. Burko. Homogeneous spacelike singularities inside spherical black holes. *Ann. Israel Phys. Soc.*, 13:212, 1997.
 - [12] Andrew J. S. Hamilton and Scott E. Pollack. Inside charged black holes. II: Baryons plus dark matter. *Phys. Rev.*, D71:084032, 2005.